frontiers | Frontiers in Energy Research

TYPE Original Research
PUBLISHED 09 November 2022
DOI 10.3389/fenrg.2022.972089

OPEN ACCESS

EDITED BY
Yimin Zhou,
Shenzhen Institutes of Advanced Technology (CAS), China

REVIEWED BY
Mohamed Salem,
Universiti Sains Malaysia (USM), Malaysia
Dheeraj Joshi,
Delhi Technological University, India

*CORRESPONDENCE
Malligunta Kiran Kumar,
kiran.malligunta@gmail.com
Salah Kamel,
skamel@aswu.edu.eg

SPECIALTY SECTION
This article was submitted to Smart Grids, a section of the journal Frontiers in Energy Research

RECEIVED 17 June 2022
ACCEPTED 25 October 2022
PUBLISHED 09 November 2022

CITATION
Venkata Govardhan Rao K, Kumar MK, Goud BS, Bajaj M, Abou Houran M and Kamel S (2022), Design of a bidirectional DC/DC converter for a hybrid electric drive system with dual-battery storing energy.
Front. Energy Res. 10:972089.
doi: 10.3389/fenrg.2022.972089

Design of a bidirectional DC/DC converter for a hybrid electric drive system with dual-battery storing energy

Kambhampati Venkata Govardhan Rao[1], Malligunta Kiran Kumar[1]*, B. Srikanth Goud[2], Mohit Bajaj[3], Mohamad Abou Houran[4] and Salah Kamel[5]*

[1]Department of Electrical and Electronics Engineering, Koneru Lakshmaiah Education Foundation, Vaddeswaram, Andhra Pradesh, India, [2]Department of Electrical and Electronics Engineering, Anurag University, Hyderabad, India, [3]Department of Electrical Engineering, Graphic Era (Deemed to be University), Dehradun, India, [4]School of Electrical Engineering, Xi'an Jiaotong University, Xi'an, China, [5]Electrical Engineering Department, Faculty of Engineering, Aswan University, Aswan, Egypt

Electric vehicles are projected to play an important role in the present and ensuing transportation as global environmental and energy issues become more serious. Looking into the growing popularity of electric vehicles, we need to pay even more attention to battery energy storage systems. Electric vehicles in the traditional sense rely on a battery to provide electricity. Influential requirements (acceleration and braking) will deteriorate the battery, or it may not be feasible to use it at all in some instances, due to the battery's compactness. This paper proposes a Bidirectional DC/DC Converter topology and investigates its operation modes. The proposed converter can be used in hybrid electric vehicles. Hybrid electric vehicles use this converter type to connect a primary battery (ES1), an extra battery (ES2), and an adjustable voltage bus. Both step-up (i.e., Dual-source low-voltage powering mode) and step-down (i.e., energy-regenerating high-voltage dc-link mode) modes of operation are possible with the proposed converter, allowing bidirectional power flow. Furthermore, the model can handle the flow of electricity between any two low-voltage sources. For the proposed Bidirectional DC/DC Converter, two ways of power transmission, circuit design, and operation modes are analyzed. A MATLAB-Simulink model of the proposed, and the system is developed based on a Digital Signal Processor flow chart, and the results of the simulation as well as the performance of the system are discussed.

KEYWORDS

bidirectional dc/dc converter (BDCC), bidirectional power flow, DSP flow chart, dual battery storage, hybrid electric vehicle

1 Introduction

Changes in vehicle technology have been prompted by a shift in bias and the depletion of power sources. Advanced technology is being studied for future vehicle applications. Fuel-cell vehicle/hybrid electric vehicles (FCV/HEV) are one of these applications that is both efficient and promising. The ideal torque-speed pattern for an electric propulsion system was previously determined using vehicle dynamics (Ehsani et al., 1997). Geometries for various cars, such as HEVs, FCVs, and greater e-mobility (Emadi et al., 2005), as well as separate but equal power electronics aggressive treatment in modern vehicle power systems to meet huge vehicle loads (Emadi et al., 2006). The required full load power can be consumed with the help of a battery, fuel cell stack, and ultracapacitors using two energy management algorithms (Schaltz et al., 2009). HEV and FC vehicle research refer to energy monitoring systems and structures, information on various HEVs and Plug-in HEVs (PHEVs), and the effect of FC efficiency on control techniques (Thounthong et al., 2009; Chan et al., 2010). This research looked at battery, unmanned, and FC-based automation. Some of the hybrid ESSs (multi-device storage systems) were also investigated (Khaligh and Li, 2010). Batteries, electric motors, and power electronic systems are employed to establish the necessary current balance (Rajashekara, 2013). A dc/dc converter featuring a slew of interlocking features was devised by the team. A dc/dc converter can improve the voltage conversion efficiency for EV and DC microgrid systems (Lai et al., 2015). EV batteries require a bidirectional DC to DC converter (BDCC) to accept high voltage power from a microgrid (Lai, 2016). Primary battery storage is frequently used to activate the FC and to power the propel motor in FCV systems. Peak power is delivered as the vehicle speeds up, which helps to compensate for the FC. Super-capacitors (SCs) and other high-density components help to reduce the maximum energy non-linearities that can occur during acceleration and braking (Moreno et al., 2006). SCs may be able to store regenerated energy during slowdown and then release it to generate more electricity during propulsion. The FC stack and storage batteries get more usage out of their FCV systems with high-power density SCs (Bauman and Kazerani, 2008).

In this paper, a unique BDCC design for FCV/HEV power systems is developed using a synchronous buck-boost circuit (Jiang et al., 2013) and an interleaved voltage-double architecture (Jung et al., 2013). There are two primary methods of operation: low-voltage power from two sources and high-voltage dc-bus energy regeneration (Wu et al., 2013). The recommended converter can switch between two low-voltage sources in a buck/boost mode, autonomously. In contrast to (Farhangi and Toliyat, 2015), provided a topology that only represents a particular concept (Lin and Chao, 2013). The primary features of the recommended converter are as follows:

- Connects several dc sources with varied voltage ranges.
- Two low-voltage sources are linked *via* an ac bus and a voltage regulator.
- Reducing the stress on switch currents while increasing the static voltage gain.

Provides large voltage differences between the high and low ports, as well as a high duty cycle.

2 Basic structure for FCV/HEV

The primary power source is a low-voltage FC stack with SCs connected to FCs in parallel and is depicted in Figure 1 of a standard (FCV/HEV) (Ehsani et al., 2009) power system. The

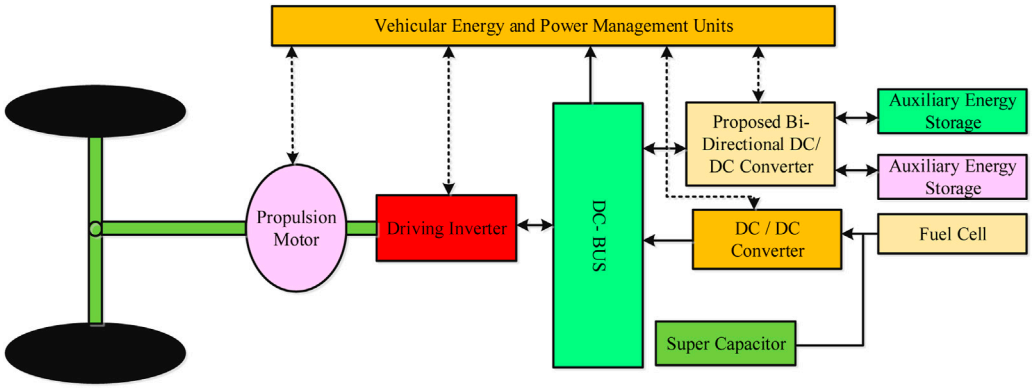

FIGURE 1
Schematic structure for an FCV/HEV power system.

TABLE 1 Literature survey.

Observation	Year	Reference
They proposed a PI controlled composite DC-DC converter is combined with a Cuk converter to provide a highly efficient electrical device for Battery Fed Electric Vehicles. In both steady-state and transient modes, the isolated DC-DC composite inverter with PI control is designed to supply enough battery voltage for dc motor control. A boost converter uses one IGBT and one MOSFET in parallel to reduce conduction loss and provide a high output voltage	2015	Rahman et al. (2015)
They presented a digital simulation of a miniature electric vehicle in action. An electric vehicle is made up of a battery, a bidirectional DC-DC converter, and a DC motor. The vehicle dynamics are considered, which represent the load torque imparted to the motor shaft. The motor and regenerative braking modes of operation are outlined, and the simulation model can mimic both modes at the same time. The energy generated during the braking phase is stored in the battery, allowing the vehicle's autonomy to be increased	2015	Azizi and Radjeai, (2015)
They proposed an electric car inter converter (EVs). This architecture, which is designed for a fully electric drive, meets propulsion needs while also allowing single-phase and three-phase AC charging. This architecture allows for considerable cost, weight, and bulk reductions when compared to current onboard integrated chargers. The new topology is theoretically studied, and simulations are used to verify its correctness	2015	Sakr et al. (2015)
This study investigates how a buck-boost converter functions as a reactive power compensation regulator for charging hybrid automobiles' batteries. This architecture will operate in buck and boost modes, depending on the rectified voltage at the input and the battery voltage at the load. Using line frequency current shaping, this work provides a simple yet effective control approach for getting the power factor closer to unity. An adaptive duty cycle control technique and an active power factor control circuit with a buck-boost converter in continuous conduction mode are used to achieve this (CCM)	2016	Mehta and Balamurugan, (2016)
To charge the batteries, a permanent magnet synchronous generator (PMSG) and multilevel inverters are required. The use of a matrix of switches to connect multiple PMSGs generates multiple voltage levels, expanding the battery filling range while the vehicle is driven at different speeds. How rapidly the battery is charged at low speeds is determined by the size of the inductor in the Buck-boost converter. The link allows the PMSGs to operate at or near full load, keeping the drive's efficiency. Under the 48–180 V AC (about 70–240-V DC) input voltage fluctuation of the PMSGs in this work, the dc output voltage is regulated at 160 V using a non-inverting buck-boost converter, reducing the power converter's complexity and scope	2016	Chauhan et al. (2016)
The function of the converters changes from boost to buck depending on the DC-link reference voltage, as seen in this article. This strategy is recommended for enhancing electric vehicle energy storage systems' optimum power savings (ESS). In driving mode, a buck-boost DC/DC converter boosts the DC-link voltage and charges the battery in braking mode. When driving in boost mode, PI control of the DC-link voltage is employed to keep the DC-link voltage constant. To avoid battery voltage fluctuations in buck mode, PI control of battery voltage is used	2016	Omara and Sleptsov, (2016)
The battery is the only source of power for electric vehicles (EVs) in the traditional sense. Severe power demands (such as acceleration and braking) may cause the battery to degrade, or even become worthless, under some circumstances because of its low power density. The high-power density of supercapacitors, on the other hand, makes them better suited for absorbing and releasing large amounts of energy. An electronic power converter system with two bidirectional dc-dc converters is designed in this work to regulate power from two energy sources (battery and supercapacitor)	2017	Herath et al. (2017)
The implementation and development of a flyback converter with a buck-boost regulator for a dc motor in a renewable energy vehicle is the focus of this research. An electric vehicle with a DC motor driven by a flyback converter and buck-boost regulator that is powered by renewable energy sources such as the sun and wind. In the current endeavour, a six-phase generator generates power from wind fans, which is then converted to DC using a six-phase converter (rectifier). By using a flyback converter in the conversion systems, ripple voltages can be reduced and the electric vehicle can run	2017	Manjunatha and Manjesh, (2017)
This article investigates the integration of a Super-capacitors (SCs) pack in a three-wheel electric vehicle, as well as the energy and power split management technique. To improve the overall productivity and efficacy of the researched vehicle, an energy-management system based on a comprehensive fuzzy logic controller technology is thoroughly examined. The proposed monitor and control methodology assumes that the battery will provide the majority of the energy while the SCs' energy levels will be intelligently maintained. The proposed technique is easy to adapt to different vehicles and modes of operation	2017	Trovão et al. (2017)
This research presents a dual-stage power converter that shares the same dc-link and will be utilized in the proposed EV rapid battery charger. The ac-dc step connects the grid with the dc link. In shunt, full-bridge voltage-source converters accept grid current and dc-link voltage in parallel Electric vehicles may be charged using a three-level unbalanced voltage-source converter	2018	Monteiro et al. (2018)
Dynamic Programming (DP) has been used to build an optimization objective function for a powerful strategic approach for coaxial series twin motor coupled propulsion systems in this work. Multiple methodologies and driving cycles are used to test the powertrain simulation model in MATLAB. The new proportional control strategy is more successful than the traditional proportional control method, which simply distributes the torques of the two induction vehicles based on default ratios	2018	Wang et al. (2018)
An onboard battery charger (OBC) for plug-in electric cars that utilizes a single-phase low-voltage (LV) LV battery charging circuit is used in this study to decouple active power. All three modes of operation can utilize the same transformer, switches, and capacitors on the OBC. Low-frequency power ripple is eliminated by the LV battery charging circuit in grid-to-vehicle and grid-to-vehicle modes. You can utilize smaller film capacitors at the DC connections point instead of larger ones. HV and LV batteries can be isolated from each other using the DC-DC converter DAB.	2018	Nguyen et al. (2018)
They developed an off-board charging station based on a dual active bridge (DAB) converter for charging multiple electric vehicle batteries. The deployment of a feature that improves power quality at the utility has reduced grid utility expenses and charging station owners' revenues	2019	Prajapati and Maurya, (2019)
Single motor direct drive and multi-speed gearboxes, which are both widespread in domestic battery-electric buses, have problems such as low overall efficiency and power interruption while shifting, according to this research. According to the	2019	Gao et al. (2019)

(Continued on following page)

TABLE 1 (*Continued*) Literature survey.

Observation	Year	Reference
findings of this study, elevated battery electric vehicles use a dual-motor system. The concept of minimal demand electric power is used to establish the switching threshold of an electric drive system's numerous load modes		
Improved motor efficiency in daily driving is achieved without the need for additional manufacturing or control complexity, conserving battery energy and lowering the cost of production. Mathematics and statistics are used to first break down a normal single propulsion motor into two different components with permanently engaged gears to calculate motor efficiency and the recommended powertrain's specifications. Dynamic powertrain simulation with Simulink/Simscape is used to create and test a cost-effective shifting strategy and dynamic torque management	2019	Ruan and Song, (2019)
Around the world, hybrid (HEVs) and electric (EVs) vehicles are growing more popular. Because of their great energy density, lithium-ion batteries are often used in these vehicles. Battery management systems (BMSs) are also required, as they rely on continuous real-time monitoring and control to ensure safe operation. The BMS determines the exact State of Charge (SOC) and Health Status (SOH). This requires recognizing and updating battery models at different stages of their lives, from the new to the elderly. Using a third-order equivalent circuit-based charging mechanism, this research proposes a dual strategy for both parameter and SOC estimates	2020	Rahimifard et al. (2020)
The purpose of this study is to create a stationary battery energy storage system (ESS) by combining used batteries from different electric vehicles (EVs), For batteries with nonoverlapping specs, two types of abandoned EVs in different situations were defined. The health and projected electrical properties of these recovered EV batteries are assessed and compared. To strike a compromise between dependability, performance, size, a modular battery ESS with a dual-feed design was developed. The modular construction allows for increased capacity and voltage level management flexibility, as well as easier battery replacement	2020	Fong et al. (2020)
They proposed the usage of double switching modulation techniques for bidirectional buck-boost converters. The buck-boost technique is utilized as the power converter design in electric automobiles (EVs) and hybrid electric vehicles (HEVs) to connect a storage system to a DC-link (HEVs). In the event of a DC-link short-circuit, this design can protect energy storage devices. The proposed control technique reduces the converter's switching losses while using a typical modulation scheme and enhances the system's dynamic response by modifying the static characteristics. Simulations are used to validate the intended control	2020	Georgious et al. (2020)
Electric cars (EVs) are quickly gaining popularity. The transformation of the automotive industry to charging electric vehicles is a major stumbling block in this era. In addition to the apparent limitations of a single charge, range concerns remain an unsolved problem. Dynamic wireless charging while you're out and about could offer some support around. The buck-boost converter is required to adjust the charging voltage for PV and dynamic recharging due to variables like speed, ground clearance (different manufacturers of EVs), misalignment, and others. The (DIBBC) small-signal concept is applied to produce a controller for three switches	2021	Nayak et al. (2021)
They developed a way for lowering charging time by using a dual battery charging mechanism. Several cells work together to create a complete battery in the recommended dual battery charging method. A switch divides the battery into two-halves during charging, and two chargers charge the battery from both sides to full charge. When the battery is fully charged, i.e. up to the predetermined point, it automatically disconnects from the charger and reunites when the battery falls below the set limit. When this method is used, the battery charging time is cut in half when compared to traditional charging methods. This approach employs a display board to display the battery's current, voltage, and charging status, which assists in battery performance monitoring	2021	Kharade et al. (2021)
To use a supercapacitor to establish a dual-energy source system and reduce power battery performance and protect the power battery from high current impact to lengthen the service life of electric vehicles with a single energy source. Dual-energy source systems benefit from the rule- and fuzzy-control-based energy management. CRUISE and MATLAB/Simulink software models are used to evaluate the strategy's effectiveness	2021	Lu et al. (2021)

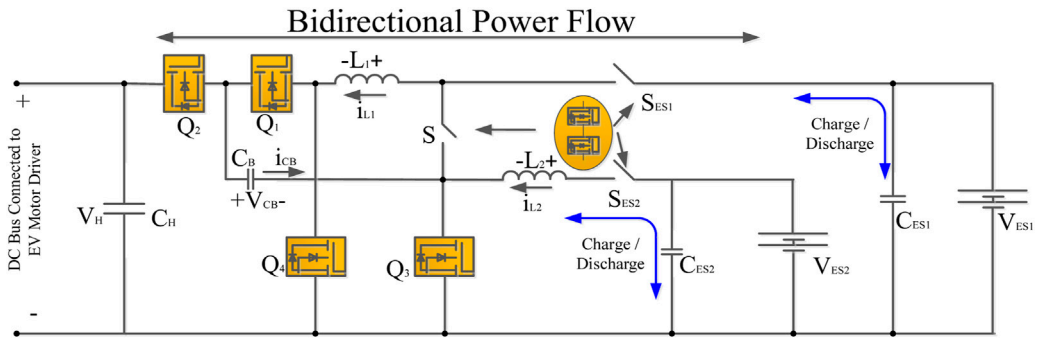

FIGURE 2
BDCC proposed architecture including dual battery storage.

TABLE 2 Devices' current state of operation for various operating modes.

Modes of functioning	On	OFF	Control switch	Synchronous rectifier (SR)
Twin-source low-voltage powering mode (accelerating, $x_1 = 1$, $x_2 = 1$)	S_{ES1}, S_{ES2}	S	Q_3, Q_4	Q_1, Q_2
Energy-recovery method for high-voltage dc buses (Braking, $x_1 = 1$, $x_2 = 1$)	S_{ES1}, S_{ES2}	S	Q1, Q2	Q_3, Q_4
Twin-source buck mode with low voltage (ES1 to ES2, $x_1 = 0$, $x_2 = 0$)	S_{ES1}, S_{ES2}	Q_1, Q_2, Q_4	S	Q_3
Dual-source low-voltage boost mode (ES1 to ES2, $x_1 = 0$, $x_2 = 0$)	S_{ES1}, S_{ES2}	Q_1, Q_2, Q_4	Q_3	S
The shutdown of the system	—	SES1, SES2	—	—
		Q_1, Q_2, Q_3, Q_4		

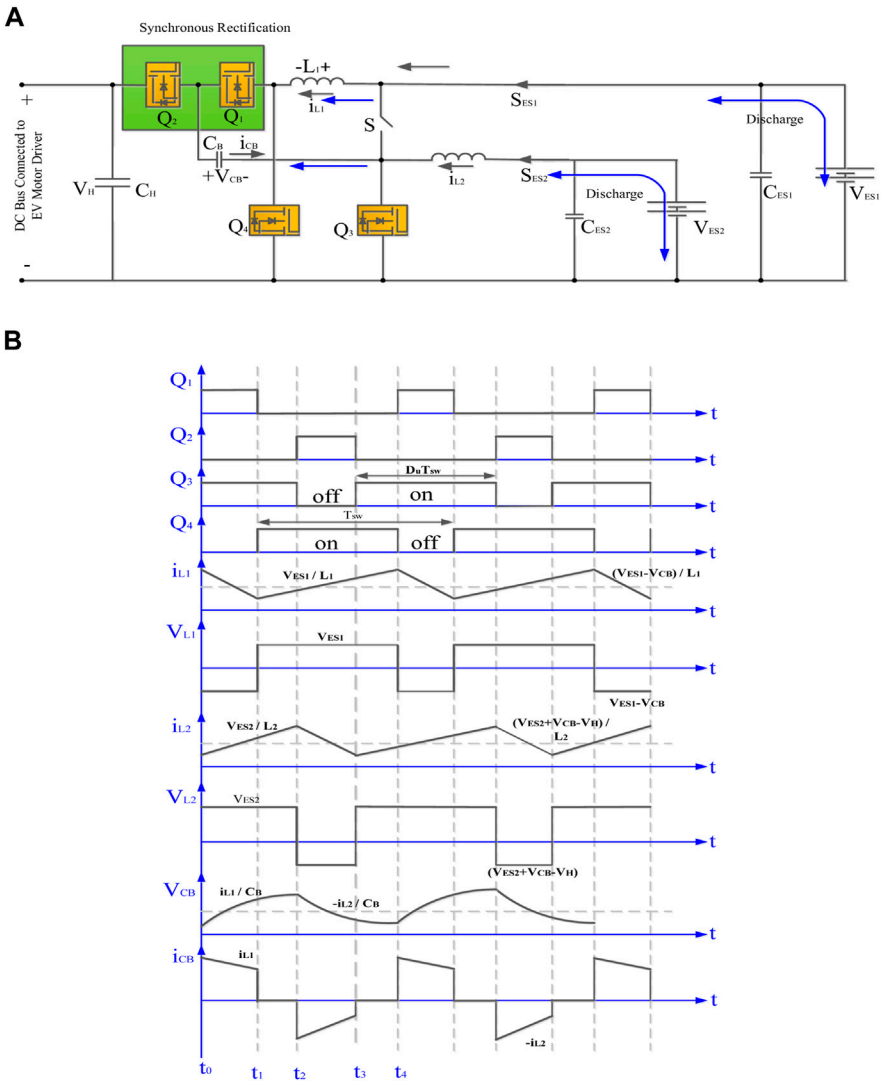

FIGURE 3
The proposed BDCC's dual-source low-voltage powering mode: **(A)** Circuit design **(B)** Stable pattern.

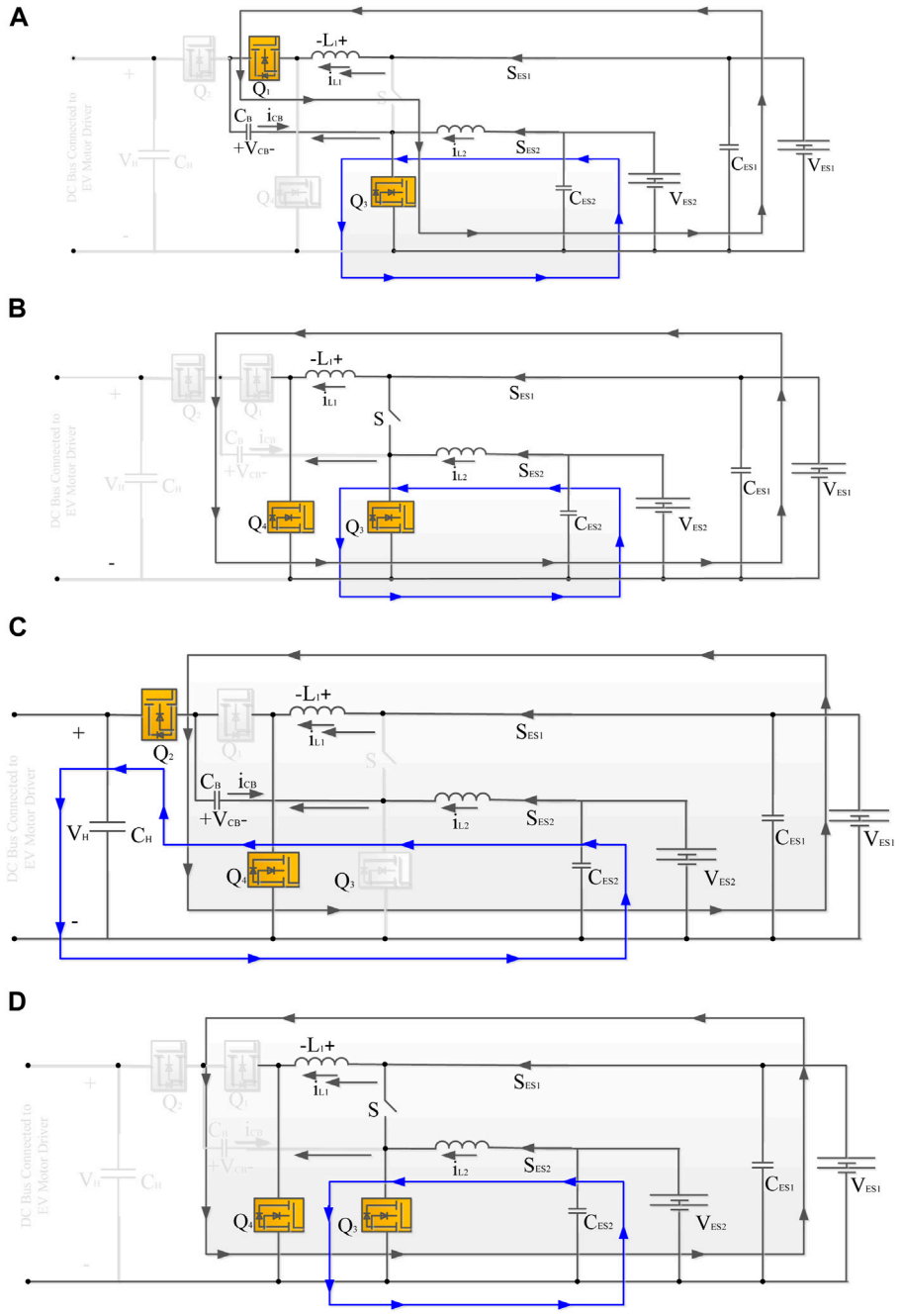

FIGURE 4
The proposed BDCC's circuit states for the dual-source low-voltage powering levels. **(A)** Level 1**(B)** Level 2 **(C)** Level 3 **(D)** Level 4.

propulsion motor can be powered by the dc-bus voltage that is generated by the driving inverter's dc/dc power components (Haihua and Khambadkone, 2008). Even though the vehicle work to expand design based on ES2, ES1 is utilized as the primary energy storage system medium for peak power generation. It is used to connect the operational inverter's dc bus to dual-energy storage. Several BDCC switches have been distributed to supply particular voltages to loads while controlling power flow between several sources (Tao et al., 2008). Overall cost, mass, and power use are all reduced. The two categories of BDCCs are isolated and non-isolated BDCCs (Bhattacharya et al., 2009).

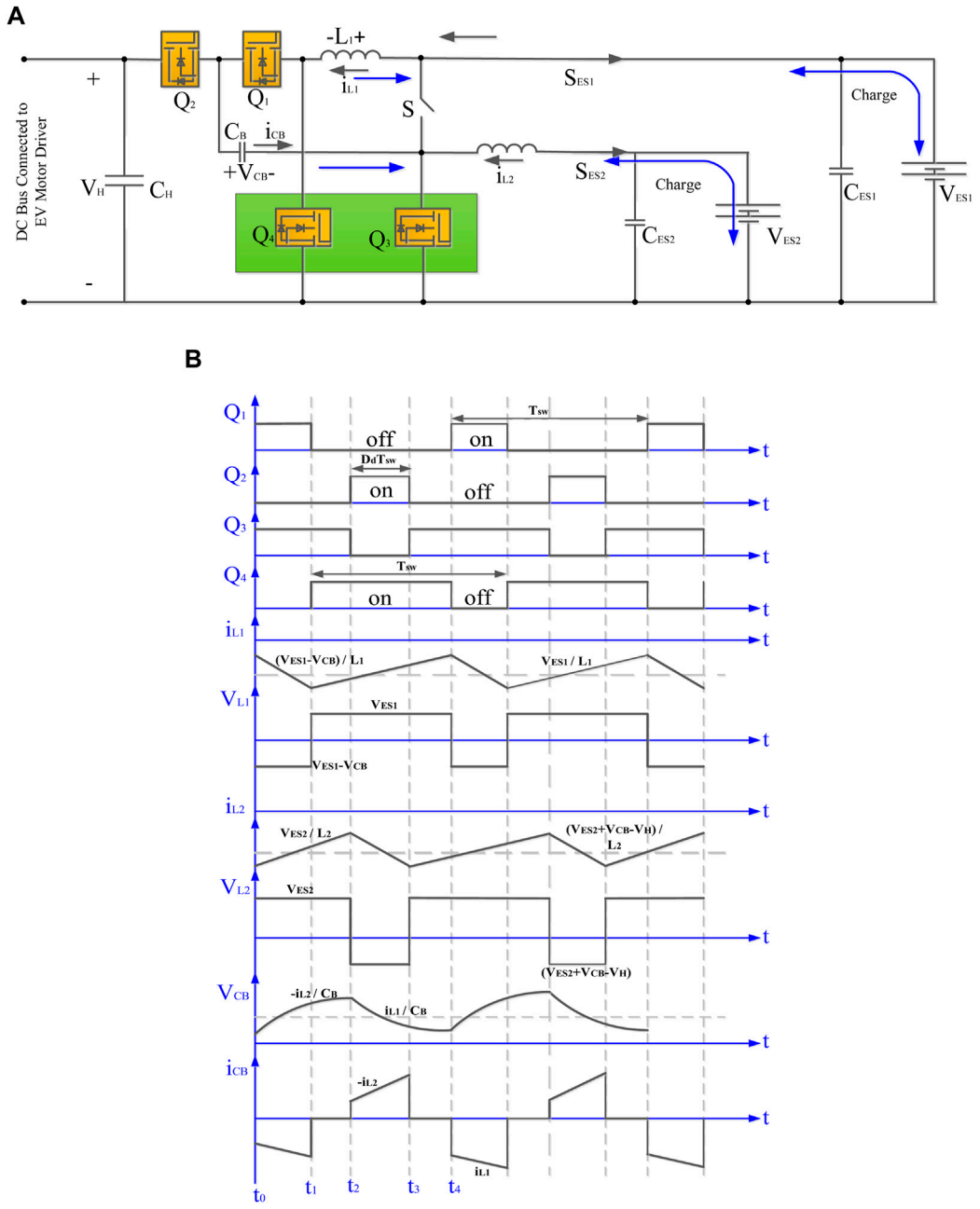

FIGURE 5
The proposed BDCC's energy-regenerating high-voltage dc-link mode: **(A)** Circuit design **(B)** Stable pattern.

Electrochemical cells are isolated from one another by using high-frequency transformers in isolated converters All other isolated multiport BDCC topologies, including hop, half or full-bridge circuits, double-active bridges, and other variations, have also been investigated (Krishnaswami and Mohan, 2009). BDCCs that are not isolated have a greater EV success rate than isolated BDCCs (Liu and Chen, 2009). Renewable energy sources, a battery storage system, and a load can all be powered simultaneously *via* the three-port non-isolated MIMO converter, which utilizes all these converter types. The three double-input converters developed in (Gummi and Ferdowsi, 2010) use a single-pole triple-throw switch and only one inductor. (Zhao et al., 2012). described a modular non-isolated dc MIMO converter. The

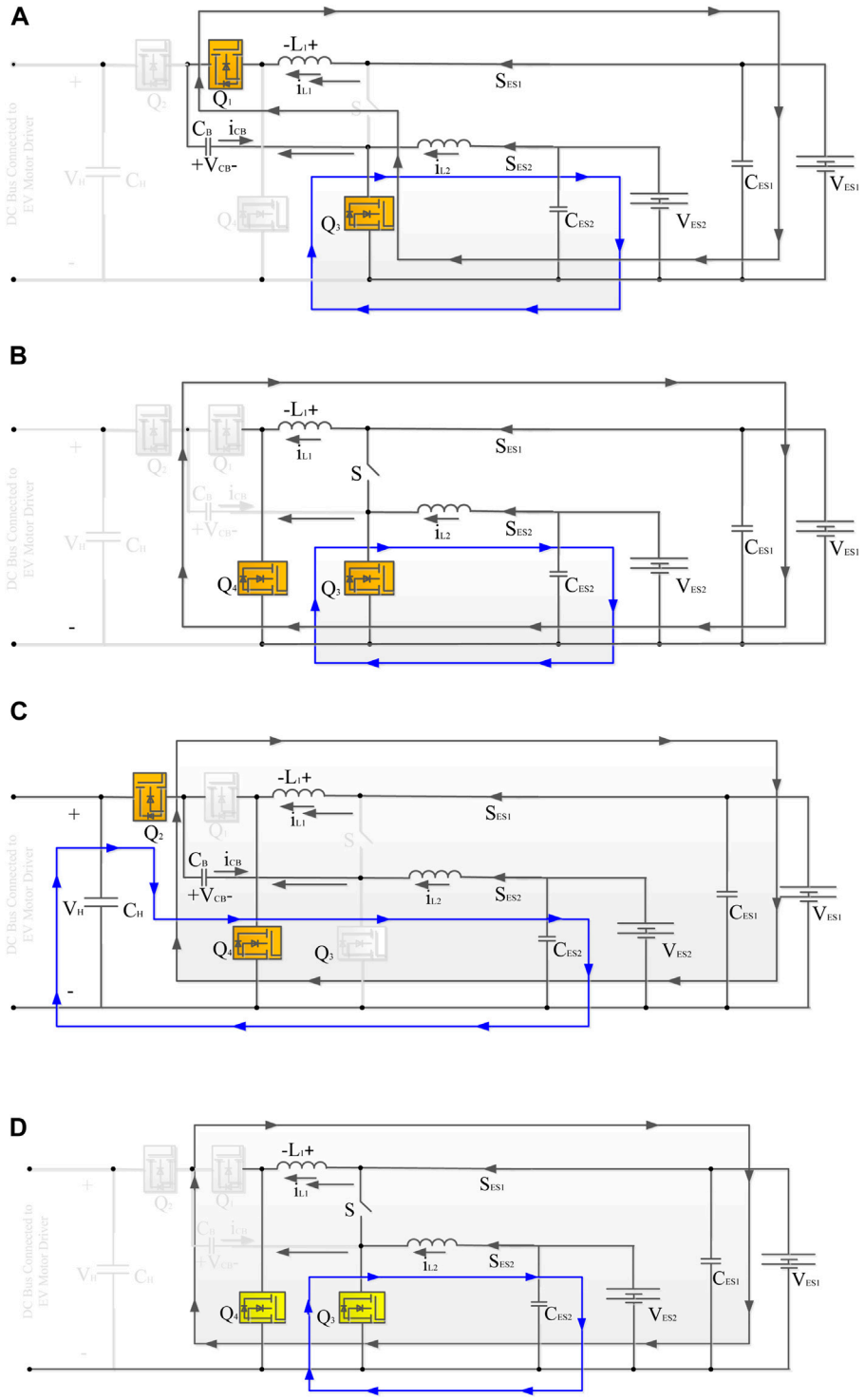

FIGURE 6
The proposed BDCC's circuit states for the energy-regenerating high-voltage dc-link levels: **(A)** Level 1**(B)** Level 2 **(C)** Level 3 **(D)** Level 4.

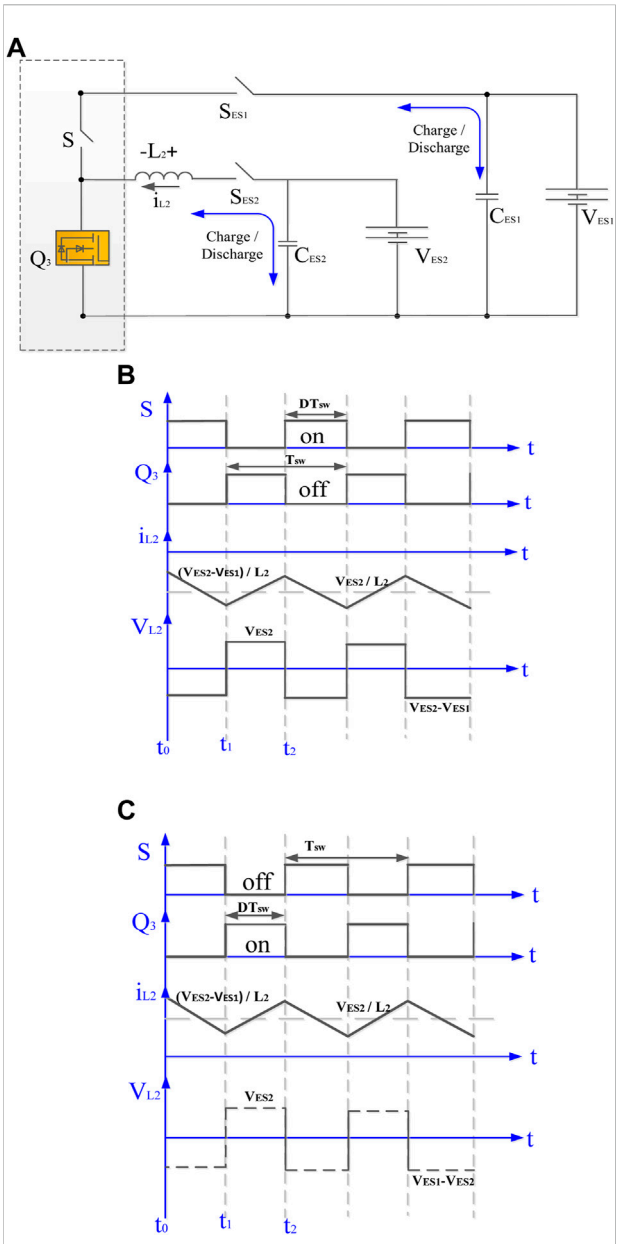

FIGURE 7
The proposed BDCC's low voltage dual-source Buck/Boost mode: **(A)** Circuit architecture **(B)** Steady-State patterns in Buck mode **(C)** Boost mode steady-state patterns.

fundamental boost circuit was improved and integrated into this converter, which is used to hybridize sustainable energy sources in electric vehicles.

2.1 Literature survey

Some of the most important references with their observation methods are listed in Table 1.

The remaining part of the paper is laid out as follows. The proposed BDCC's structure, as well as its operation modes, are explored and detailed in section 3. Section 4 describes the converter's control system, and Section 5 depicts the simulation results for various operation modes. Conclusions and future work are presented at the end of the paper.

3 Topology and operation modes

The elevated dc bus voltage (V_H, V_{ES1}, and V_{ES2}), basic stored energy, and supplemental energy storage are shown in Figure 2 of the BDCC design (ES2), The current circuits of ES1 and ES2 are turned on and off by two bidirectional power switches (S, S_{ES1} and S_{ES2}) in the converter's layout (Kharade et al., 2021).

A charge-pump capacitor (CB) with four active switches (Q_1, Q_2, Q_3, Q_4) and two-phase inductors (L_1, L_2) improves the dynamic voltage gain between two low-voltage dual sources (V_{ES1}, V_{ES2}) and the higher-voltage bus (V_H). By adding an extra CB, switching voltage stress is reduced, and a high duty ratio is no longer required.

Table 2 depicts all the conductivity levels of such power devices involved in each working model to demonstrate the concept for the proposed converter (Moradisizkoohi et al., 2019). As a result, the four functional states are illustrated as follows to aid comprehension.

3.1 Twin-source low-voltage powering mode

Stable patterns for the converter are shown in Figure 3, for dual-source low-voltage powering, Figure 3A. In the circuit, S_{ES1}, and S_{ES2} are activated while controller S is deactivated. The V_{ES1} and V_{ES2} provide power to loads as well as a dc bus. The controllers Q_3 and Q_4 switch at a 180° phase difference in this mode, while the remaining Q_1 and Q_2 act as synchronous rectifiers (SR).

More than half of the duty ratio allows access to four circuit levels as indicated in Typical Patterns Figure 3B. (As depicted in Figure 4). According to the state of the BDCC and the active switches, dual-source low-voltage powering mode operation can be described as follows.

3.1.1 Level 1 [$t_0 < t < t_1$]

(1-Du)Tsw is the duration of the operation. The MOSFETsQ_1, Q_3, and Q_2, Q_4 are active throughout the period, whereas Q_2, Q_4 are dormant. The difference between V_{ES1} and V_{CB} is the voltage across L_1. As a result, i_{L1} decreases linearly from its basic value, whereas L_2 is charged by V_{ES2}in Figure 4A. Therefore, the inductor current rises linearly (Jang and Jovanovic, 2007). The relevant Eqs (Ehsani et al., 1997; Emadi et al., 2005)

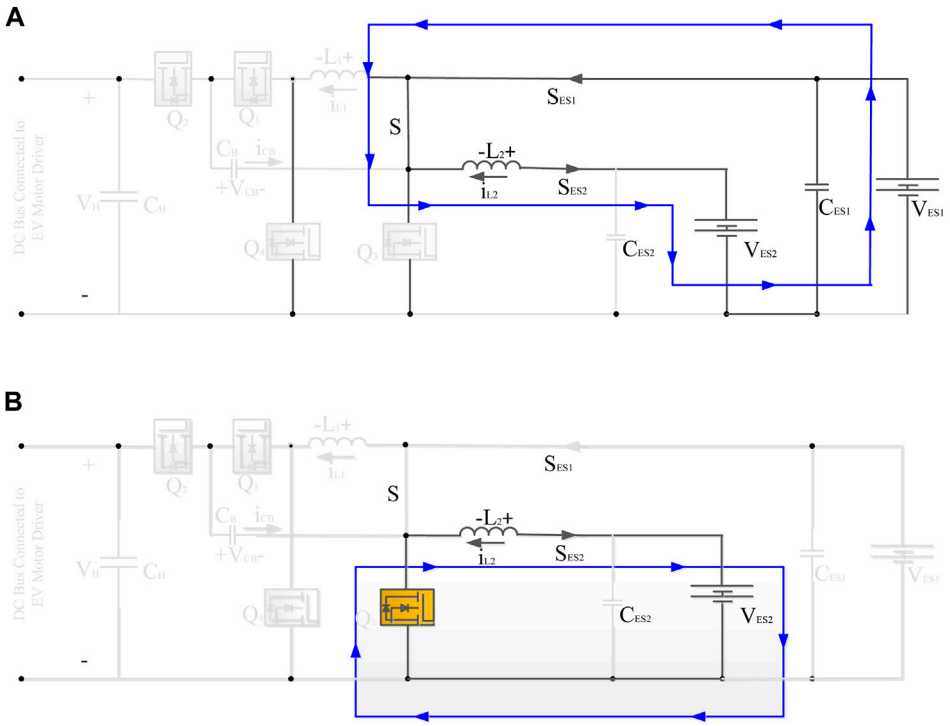

FIGURE 8
The proposed BDCC circuit states for the low voltage dual-source buck mode **(A)** level 1 and **(B)** level 2.

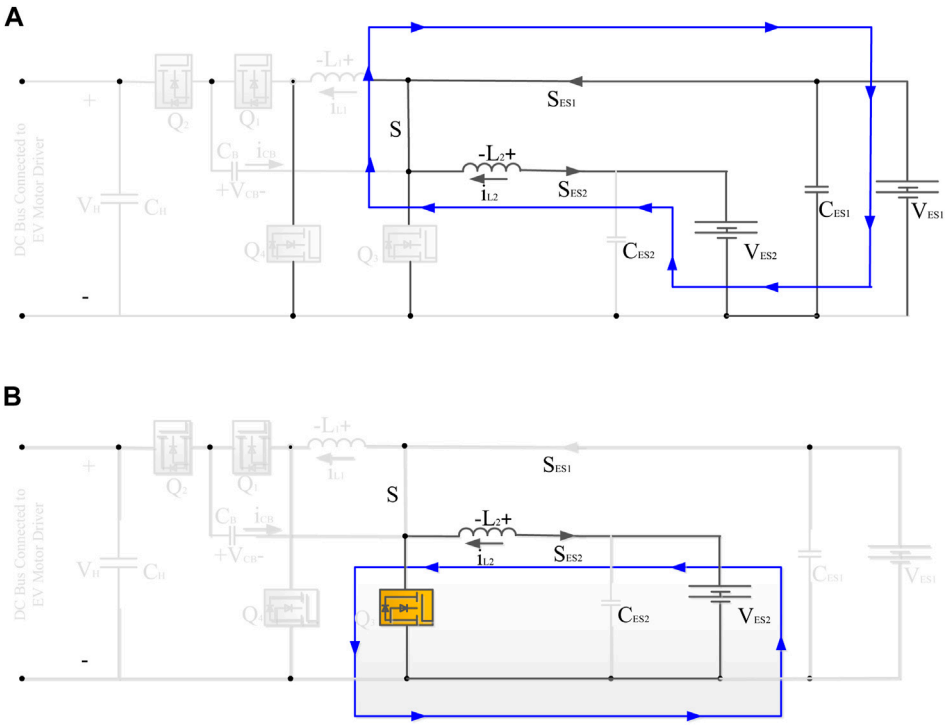

FIGURE 9
The suggested BDCC circuit states for the low voltage dual-source boost mode **(A)** level 1 and **(B)** level 2.

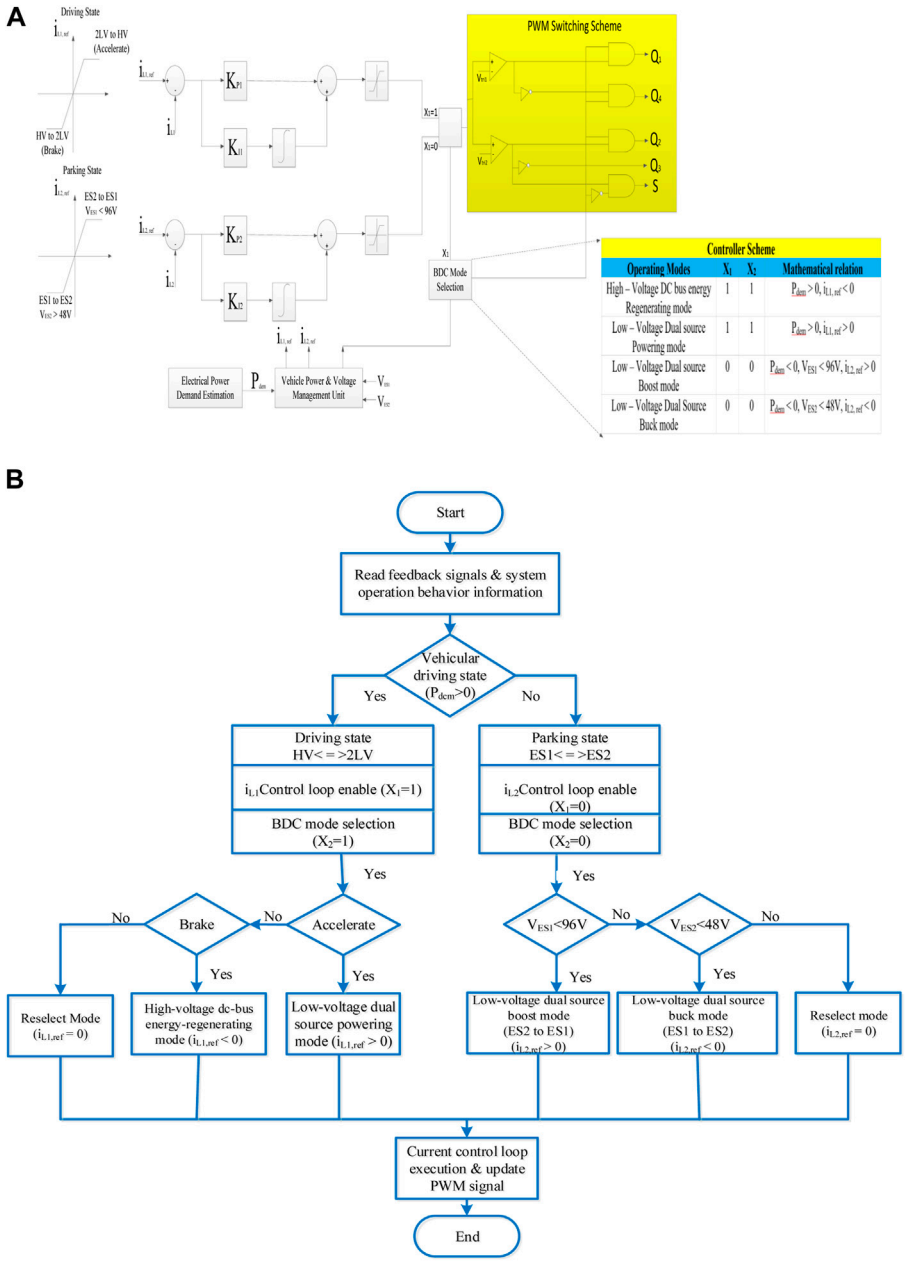

FIGURE 10
(A) Block diagram of the closed-loop control method; **(B)** designed DSP flowchart of the proposed BDCC's multiple operating modes (Lai et al., 2018).

$$L_1 \frac{di_{L1}}{dt} = V_{ES2} - V_{CB} \quad (1)$$

$$L_2 \frac{di_{L2}}{dt} = V_{ES2} \quad (2)$$

3.1.2 Level 2 [$t_1 < t < t_2$]

The length of time is (Du-0.5). In this state T_{sw}, transistorsQ_3 and Q_4 are active, while Q_1 and Q_2 are inactive. Low-side voltages V_{ES1} and V_{ES2} are located between inductors L_1 and L_2,

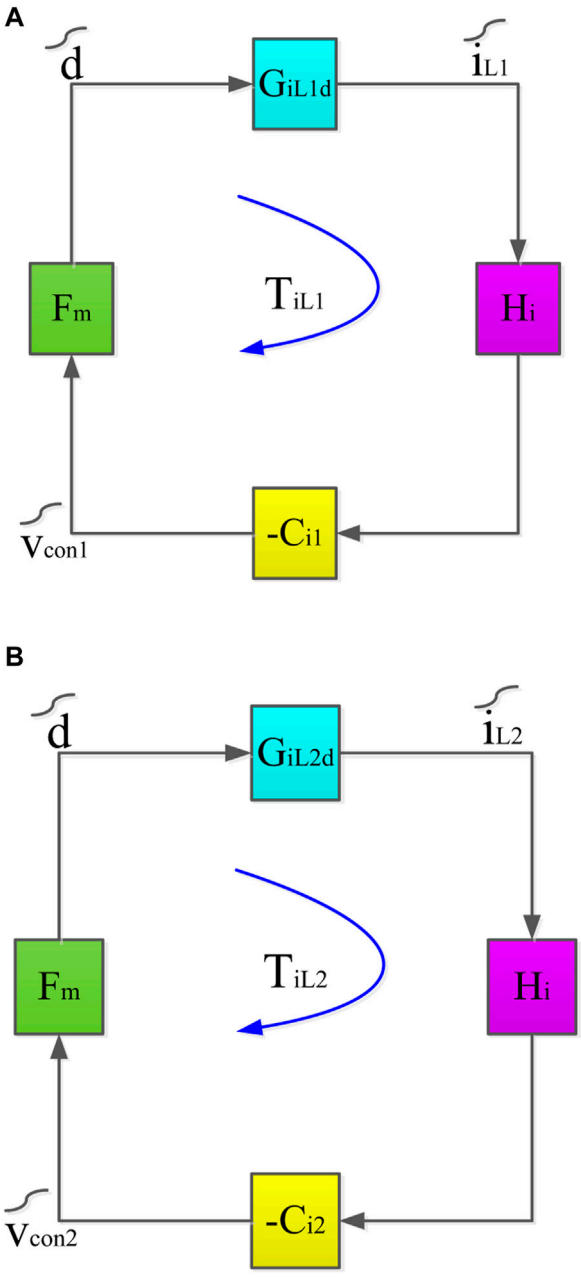

FIGURE 11
Diagrams demonstrating a closed-loop control method for **(A)** the energy from an energy-regenerating high-voltage dc-link mode and **(B)** the Dual-source low-voltage powering mode.

respectively, rising inductor currents linearly and initiating energy storage as indicated in Figure 4B. The voltages across inductors L_1 and L_2 may be expressed as Eq. (Emadi et al., 2006; Schaltz et al., 2009).

$$L_1 \frac{di_{L1}}{dt} = V_{ES1} \tag{3}$$

$$L_2 \frac{di_{L2}}{dt} = V_{ES2} \tag{4}$$

3.1.3 Level 3 [$t_2 < t < t_3$]

(1-Du)Tswis the duration. The transistorsQ_1 and Q_3 are active throughout this time, whereas Q_2 and Q_4 are idle, in Figure 4C. The voltage expressions are (Thounthong et al., 2009; Chan et al., 2010)

$$L_1 \frac{di_{L1}}{dt} = V_{ES1} \tag{5}$$

$$L_2 \frac{di_{L2}}{dt} = V_{CB} + V_{ES2} - V_H \tag{6}$$

3.1.4 Level 4 [$t_3 < t < t_4$]

The duration is (Du-0.5)Tsw in this interval the transistorsQ_3 and Q_4 are active and Q_1 and Q_2 are inactive in Figure 4D. The voltages expressions can be written as Eqs (Khaligh and Li, 2010; Rajashekara, 2013)

$$L_1 \frac{di_{L1}}{dt} = V_{ES1} \tag{7}$$

$$L_2 \frac{di_{L2}}{dt} = V_{ES2} \tag{8}$$

3.2 Energy-regenerating mode for high-voltage DC-Bus

Electricity is continuously supplied to and retrieved from the motor drive in this mode. There is a possibility that the regeneration power will exceed the battery's ability to absorb it. A Rechargeable battery-powered storage device is an excellent option for this maximum electricity (Lai et al., 2018). Figure 5 (a) presents the BDCC circuit architecture and standard state pattern in the energy-regenerating high-voltage dc-link mode.

The inductive current may be adjusted with the 180^0 phase angle using active switchesQ_1, Q_2. To increase the conversion efficiency illustrated in Figure 5, the remaining switchesQ_3, and Q_4 will operate as SR shown in Figure 5A, the stable waveforms duty ratio is less than 50%, as shown in Figure 5B, with these four various levels being achievable and stated as follows.

3.2.1 Level 1 [$t_0 < t < t_1$]

The period is D_dT_{sw}, and Q_1 and Q_3 are active, while Q_2 and Q_4 are inactive. The variation between the lowered voltage V_{ES1} and the charge-pump voltage V_{CB} is equal to the voltage across L1, therefore the inductor current i_{L1} steadily drops from its beginning value seen in Figure 6A. The energy source V_{ES2} also charges inductor L_2, causing the inductor current to expand linearly. The following are the important Eqa (Lai et al., 2015; Lai, 2016):

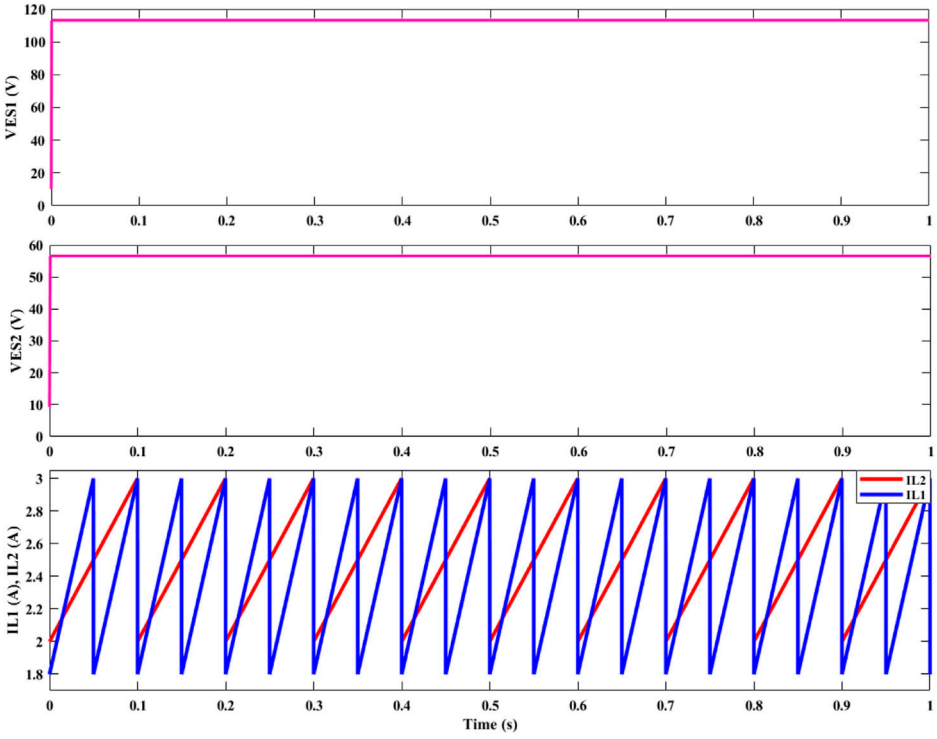

FIGURE 12
Output voltage and inductor currents for a higher-potential dc-bus power-regenerating mode were measured.

$$L_1\frac{di_{L1}}{dt} = V_{ES1} - V_{CB} \quad (9)$$

$$L_2\frac{di_{L2}}{dt} = V_{ES2} \quad (10)$$

3.2.2 Level 2 [$t_1 < t < t_2$]

The length of time is (0.5-D_d) The MOSFETsQ_3 and Q_4 are active in this scenario, whereas Q_1 and Q_2 are inactive. Inductor currents i_{L1} and i_{L2} develop linearly as L_1 and L_2 are positive in relation to the low-side voltages V_{ES1} and V_{ES2}, as illustrated in Figure 6B are Eqs 11, 12.

$$L_1\frac{di_{L1}}{dt} = V_{ES1} \quad (11)$$

$$L_2\frac{di_{L2}}{dt} = V_{ES2} \quad (12)$$

3.2.3 Level 3 [$t_2 < t < t_3$]

The duration is D_dTsw in this scenario, and the transistorsQ_1 and Q_3 are inactive, while Q_2 and Q_4 are active from Figure 6C. The application of a positive low-side voltage V_{ES1} across L_1 causes i_{L1} to expand linearly from its original value. Because of the discrepancy between the high-side voltage V_H, the charge-pump voltage V_{CB}, and the low-side voltage V_{ES2}, the voltage across L_2 is also negative. The relevant Eqs [13–14] are as follows

$$L_1\frac{di_{L1}}{dt} = V_{ES1} \quad (13)$$

$$L_2\frac{di_{L2}}{dt} = V_{ES2} + V_{CB} - V_H \quad (14)$$

2.2.3. Level 4 [$t_3 < t < t_4$]: The period is (0.5-D_d)T_{sw} in this case, and the switchesQ_3 and Q_4 are active, while Q_1 and Q_2 are passive shown in Figure 6D are Eqs 15, 16

$$L_1\frac{di_{L1}}{dt} = V_{ES1} \quad (15)$$

$$L_2\frac{di_{L2}}{dt} = V_{ES2} \quad (16)$$

3.3 Twin-source low-voltage buck/boost mode

Figure 7 shows that the energy is exchanged from the primary store to the improved storage. In this phase, the converter is a single-leg bidirectional buck-boost.

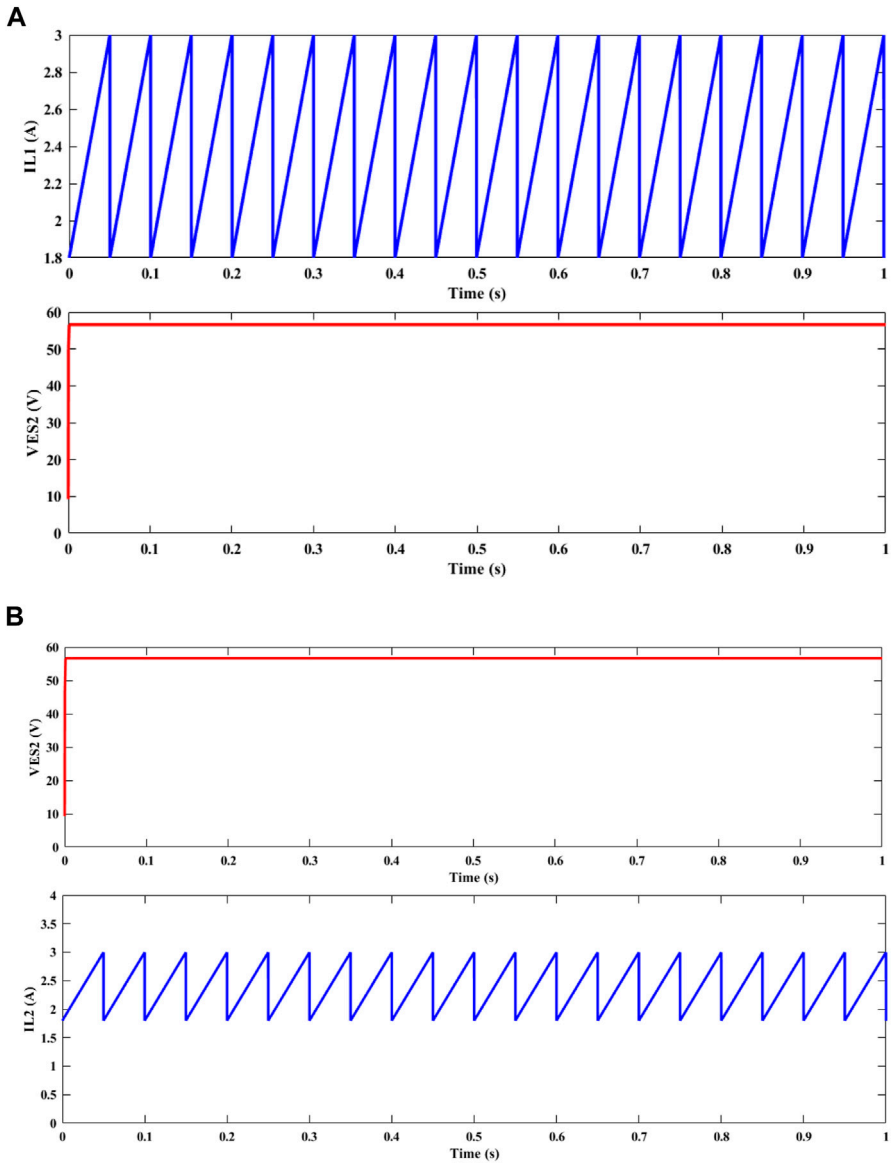

FIGURE 13
Low-voltage dual-source buck/boost mode, waveforms of output voltage, and inductor currents: **(A)** Boost Mode; **(B)** Buck Mode.

According to Figure 8, the active bidirectional switch S's duty cycle can be altered, which triggers the buck converter to switch power over to secondary energy storage.

According to Figure 9, primary and supplementary energy storage are both boosted when the transistor'sQ$_3$ duty cycle is adjusted to signal that it is in "boost operation mode.

4 Converter control

The BDC controller of the converter control system is depicted in Figure 10A, which contains a vehicular strategic management level. Figure 10B represents a real-time DSP flowchart used to test various working modes of the proposed BDCCs.

The regulation of flow in two ways from a lower potential source at two sides and a higher potential dc bus is shown in Figure 10A by using the current reference ($i_{L1,\ ref}$). This BDCC topology's uniform average current sharing means that i_{L2} is nearly identical to i_{L1} regulated average inductor current. In distinction, the reference at current $i_{L2,\ ref}$ is employed for regulating the flow of power from primary and secondary energy storage systems. By using the triangular wave as one of the inputs, such as v_{tri1} and v_{tri2}, the PWM ON and OFF method turns the total time dictated by a distinct selection of

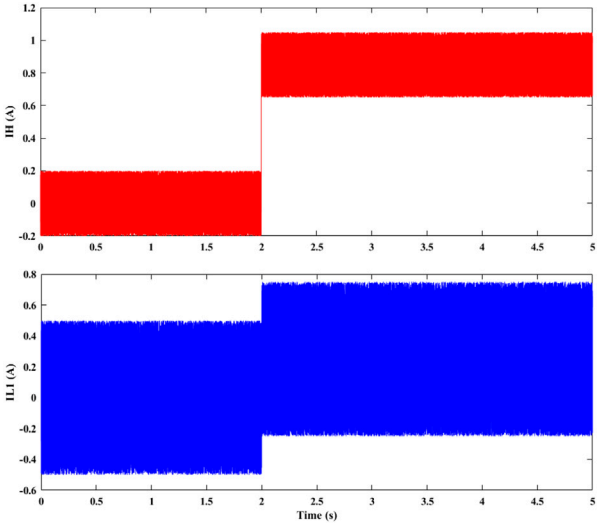

FIGURE 14
Simulation patterns of a managed current change in step in lower-potential dual-source powering mode (i_H altered from 0 to 0.85 A; i_{L1} changed from 0 to 2.5 A).

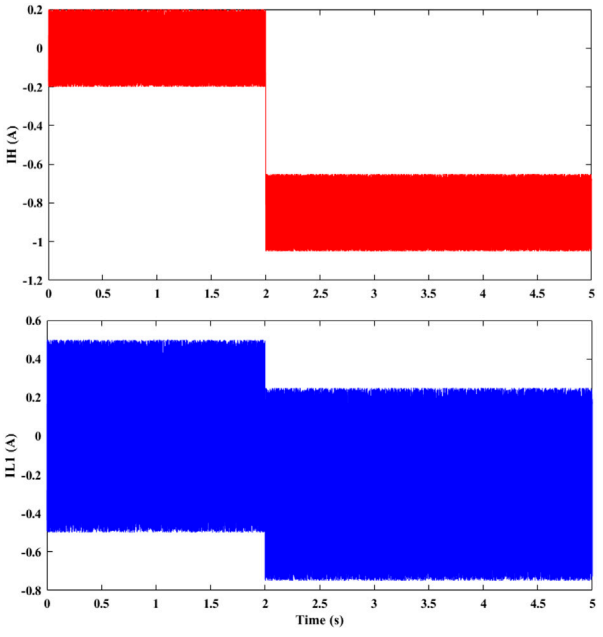

FIGURE 15
Simulation patterns of managed changes in current at step level in the higher-potential dc-bus power-regenerating mode (i_H altered from 0 to −0.85 A; i_{L1} changed from 0 to −2.5 A).

switches for switching ON gate control of power switches. It then chooses one of two current references, $i_{L1,\ ref}$ or $i_{L2,\ ref}$, to regulate the switches (S, Q_1-Q_4) using PI or more complex approaches.

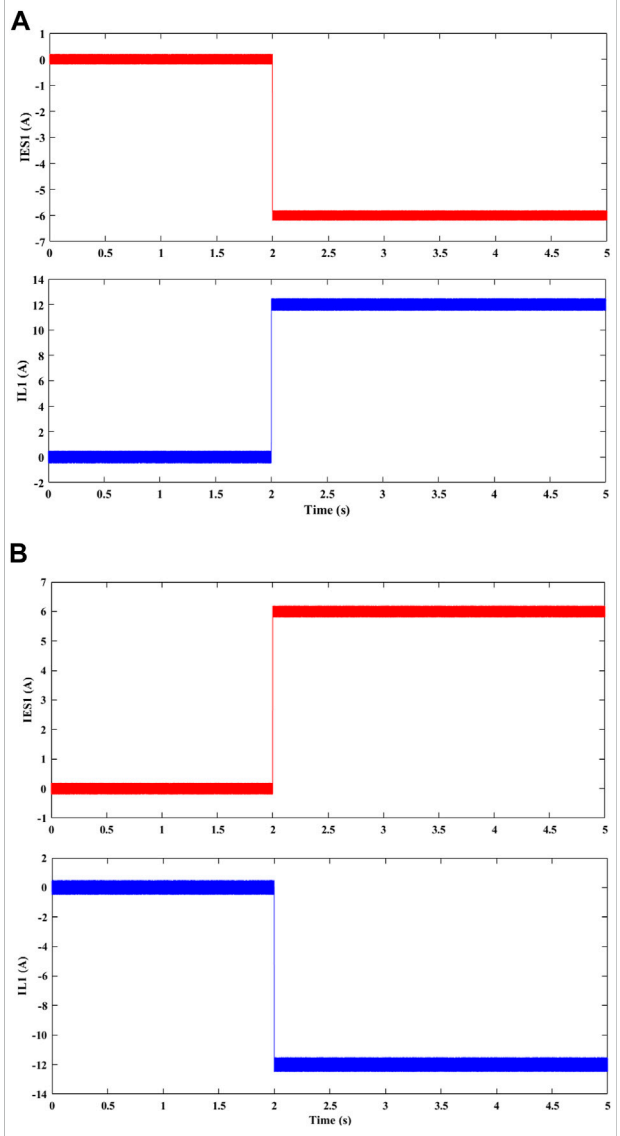

FIGURE 16
Simulation patterns of a managed step change in current in lower potential dual-source **(A)** Boosting Mode and **(B)** Buck Mode.

Figure 10B depicts the switching mode strategy, which is further detailed in the following diagram. To begin, the controller is in the i_{L1} control loop ($x_1 = 1$) while the vehicle is in driving mode ($P_{dem}>0$), and the switch button which can be controlled is mentioned in Table 2 (the vehicle is accelerating ($i_{L1,\ ref}>0$, HV to 2 LV) or braking ($i_{L1,\ ref}$ 0, 2 LV to HV). If none of these circumstances applies, the following mode switching judgment will be processed using reselect mode. Furthermore, the controller is in the i_{L2} control loop ($x_1 = 0$) while the automobile is in the parking state (Pdem<0), and the switches are controlled as shown in Table 2. In this situation, the voltages of V_{ES1} (96 V) and V_{ES2} (72 V) influence mode switching (48 V). The mode is a low-voltage dual-source

TABLE 3 Illustrating the difference in the performance among a wide range of converters.

Items	Topology				
	Hintz et al. (2015)	Lin and Chao, (2013)	Chen et al. (2013)	Wai and Chen, (2014)	Proposed
Switching control structure	single-phase	single-phase	single-phase	four-phase	two-phase
Bidirectional power flow	Yes	No	No	Yes	Yes
Output ripple	Medium	High	Low	Low	Low
Number of PWM controlled switches	6	5	4	8	6
Passive components	5	7	15	4	6
Maximum conversion efficiency	91.5%	94%	93%	95%	97.25%
High-side voltage	300 V	400 V	540 V	200 V	430 V
Low-side voltages	V_{ES1}: 125 V	V_{ES1}:30–50 V	V_{ES1}: 240–300 V	V_{ES1}: 42–63 V	V_{ES1}: 96 V
	V_{ES2}: 144 V	V_{ES2}: 50–100 V	V_{ES2}: 240–300 V	V_{ES2}: 48 V	V_{ES2}: 48 V

boost ($i_{L2,\ ref}>0$, V_{ES2} to V_{ES1}) while $V_{ES1}<96$ V is present, and a low-voltage dual-source buck ($i_{L2,\ ref}>0$, V_{ES1} to V_{ES2}) when $V_{ES2}<48$ V is present. If none of these requirements is fulfilled, the following mode switching judgment is processed using reselect mode. Based on the state-space averaging approach, only regulators with two closed-loop are designed to regulate the power flow in four conditions.

From Figure 11: the notations are

Fm: Indicates the PWM generator's constant gain.

G_{iL1d}: Represents the ON and OFF cycle to current at inductor i_{L1} conversion function.

G_{iL2d}: ON and OFF cycle to current at inductor controller transfer function.

Hi: Gain of the current sensor.

C_{i1} and C_{i2}: Depict the inductor current controllers' transfer function

Figures 11A,B depict closed-loop control block designs for lower-potential sources at dual end buck or boost (LV to HV) and higher-potential dc-bus power-regeneration modes, respectively.

5 Simulation results

Simulations are performed to check the performance of the suggested model, with the parameter components of C = 10μF, L = 250 mH, and V = 48V, 96 V and DC motor is assumed as an electric vehicle.

The model simulation is done in MATLAB-Simulink. The results are presented and discussed below.

The system power transmission from the dc-bus to the main & auxiliary energy storage is depicted in Figure 12. Currents flow in the opposite direction as the input power in inductors i_{L1} and i_{L2}. VES1 and VES2 were at 96 V and 48V, respectively, on the low end.

Figures 13A,B illustrate that currents in inductors are exactly the opposite of what we can see, indicating that the model works well for both primary and secondary energy storage.

For the simulated system, these Figures 14, 15 depict the regulated current step shift waveforms in the lower potential dual-source providing and higher potential dc-bus electricity modes. The power flow was efficiently reversed, as indicated by the negative current waveforms, by changing i_H and i_{L1} currents from low-side sources to supply 360 W of power to the elevated bus, as shown in Figures 14, 15.

We may adjust the current step shift of the prototype system using these two low-voltage operation modes, low voltage boost and low voltage buck. The raised current i_{ES1} and the inductance current i_{L2} were both modified to supply 576 W of power between reduced dual sources, as depicted in Figure 16A. The negative current waveform in Figure 16B shows how the output current was effectively reversed.

Comparisons of the proposed BDCC's performance with existing models in the relevant literature are exhibited in Table 3.

Compared the proposed converter with the ones in (Lin and Chao, 2013) and (Chen et al., 2013), point out the fact that our converter includes fewer passive components. A further limitation of the other models is their inability to transfer energy in both directions. Although both (Hintz et al., 2015) and (Wai and Chen, 2014) claim to have bidirectional power flow, their best conversion efficiency is less than that of the converter suggested in this work. Furthermore, compared to the models provided in (Chen et al., 2013; Lin and Chao, 2013; Wai and Chen, 2014; Hintz et al., 2015), the proposed BDCC has a greater voltage conversion ratio.

6 Conclusion

This paper has explained the evolution of advanced bidirectional DC to DC converter topology. From BDCC, twin low voltage powering function, both the accelerating mode and braking mode

were explained. In the case of high voltage powering function buck and boost, the model has been operated by controlling the switches. Also, a novel converter control for vehicle strategic management level, designed for the proposed BDCC controller with the help of digital signal processor (DSP) flow chart representations was presented. Various power transmission methods were used to handle the recommended BDC's circuit layout, operating principles, analysis, and static voltage gains. A simulation system has been used to study and analyze the proposed BDCC topology's performance and viability. It was found that the maximum energy capacity of the four different types of lower-potential dual-source charging systems is 97%, 95%, 95%, and 96%. The outputs have shown that suggested BDCC implements an electric hybrid design in FC/HEV systems. So, Electric vehicles (EVs) will increase battery availability. To put this in context, identifying applications for a lot of power generation potentials can provide tremendous value and even help drive down the cost of storage, allowing for more sustainable inclusion into our grids.

Data availability statement

The original contributions presented in the study are included in the article/Supplementary Material, further inquiries can be directed to the corresponding authors.

Author contributions

KVGR and MKK: Conceptualization, Data curation, Formal analysis, Methodology, Resources, Software, Validation, Visualization, Writing—original draft. BSG: Data curation, Investigation, Supervision., KVGR, SK, and MB: Writing—review and editing. All authors have read and agreed to the published version of the manuscript.

Conflict of interest

The authors declare that the research was conducted in the absence of any commercial or financial relationships that could be construed as a potential conflict of interest.

Publisher's note

All claims expressed in this article are solely those of the authors and do not necessarily represent those of their affiliated organizations, or those of the publisher, the editors and the reviewers. Any product that may be evaluated in this article, or claim that may be made by its manufacturer, is not guaranteed or endorsed by the publisher.

References

Azizi, I., and Radjeai, H. (2015). "A bidirectional DC-DC converter fed DC motor for electric vehicle application," in 2015 4th International Conference on Electrical Engineering (ICEE), Boumerdes, Algeria, December 2015 (IEEE), 1–5. doi:10.1109/INTEE.2015.7416683

Bauman, J., and Kazerani, M. (2008). A comparative study of fuel-cell–battery, fuel-cell–ultracapacitor, and fuel-cell–battery–ultracapacitor vehicles. *IEEE Trans. Veh. Technol.* 57 (2), 760–769. doi:10.1109/tvt.2007.906379

Bhattacharya, T., Giri, V. S., Mathew, K., and Umanand, L. (2009). Multiphase bidirectional flyback converter topology for hybrid electric vehicles. *IEEE Trans. Ind. Electron.* 56 (1), 78–84. doi:10.1109/tie.2008.2004661

Chan, C. C., Bouscayrol, A., and Chen, K. (2010). Electric, hybrid, and fuel-cell vehicles: Architectures and modeling. *IEEE Trans. Veh. Technol.* 59 (2), 589–598. doi:10.1109/tvt.2009.2033605

Chauhan, A. K., Vakacharla, V. R., Verma, A. K., and Singh, S. K. (2016). "Multiple PMSG fed Non-inverting buck-boost converter for HEVs," in 2016 IEEE 6th International Conference on Power Systems (ICPS), New Delhi, India, March 2016 (IEEE), 1–6. doi:10.1109/ICPES.2016.7584156

Chen, Y.-M., Huang, A. Q., and Yu, X. (2013). A high step-up three-port dc–dc converter for stand-alone PV/battery power systems. *IEEE Trans. Power Electron.* 28 (11), 5049–5062. doi:10.1109/tpel.2013.2242491

Ehsani, M., Gao, Y., and Emadi, A. (2009). *Modern electric, hybrid electric, and fuel cell vehicles: Fundamentals, theory, and design*. CRC Press.

Ehsani, M., Rahman, K. M., and Toliyat, H. A. (1997). Propulsion system design of electric and hybrid vehicles. *IEEE Trans. Ind. Electron.* 44 (1), 19–27. doi:10.1109/41.557495

Emadi, A., Rajashekara, K., Williamson, S. S., and Lukic, S. M. (2005). Topological overview of hybrid electric and fuel cell vehicular power system architectures and configurations. *IEEE Trans. Veh. Technol.* 54 (3), 763–770. doi:10.1109/tvt.2005.847445

Emadi, A., Williamson, S. S., and Khaligh, A. (2006). Power electronics intensive solutions for advanced electric, hybrid electric, and fuel cell vehicular power systems. *IEEE Trans. Power Electron.* 21 (3), 567–577. doi:10.1109/tpel.2006.872378

Farhangi, B., and Toliyat, H. A. (2015). Modeling and analyzing multiport isolation transformer capacitive components for onboard vehicular power conditioners. *IEEE Trans. Ind. Electron.* 62 (5), 3134–3142. doi:10.1109/tie.2014.2386800

Fong, Y. C., Wang, D. H., Mei, J., Raman, S. R., and Cheng, K. W. E. (2020). "Study and development of Mixed Repurposing EV battery system for Stationary energy storage applications," in 2020 8th International Conference on Power Electronics Systems and Applications (PESA), Hong Kong, China, December 2020 (IEEE), 1–6. doi:10.1109/PESA50370.2020.9343967

Gao, Y., Wang, W., and Li, Y. (2019). "Optimization of control strategy for dual-motor Coupling propulsion system based on dynamic Programming method," in 2019 3rd Conference on Vehicle Control and Intelligence (CVCI), Hefei, China, September 2019 (IEEE), 1–6. doi:10.1109/CVCI47823.2019.8951627

Georgious, R., Saeed, S., Garcia, J., and Garcia, P. (2020). "Switching Schemes of the bidirectional buck-boost converter for energy storage system," in 2020 IEEE Vehicle Power and Propulsion Conference (VPPC), Gijon, Spain, December 2020 (IEEE), 1–5. doi:10.1109/VPPC49601.2020.9330869

Gummi, K., and Ferdowsi, M. (2010). Double-input dc–dc power electronic converters for electric-drive vehicles Topology exploration and synthesis using a single-pole triple-throw switch. *IEEE Trans. Ind. Electron.* 57 (2), 617–623. doi:10.1109/tie.2009.2032762

Haihua, Z., and Khambadkone, A. M. (2008). "Hybrid modulation for dual active bridge bi-directional converter with extended power range for ultracapacitor application," in Industry Applications Society Annual Meeting, Edmonton, AB, Canada, October 2008 (IAS'08 IEEE), 1–8.

Herath, N., Binduhewa, P., Samaranayake, L., Ekanayake, J., and Longo, S. (2017). "Design of a dual energy storage power converter for a small electric vehicle," in 2017 IEEE International Conference on Industrial and Information Systems (ICIIS), Peradeniya, Sri Lanka, December 2017 (IEEE), 1–6. doi:10.1109/ICIINFS.2017.8300393

Hintz, A., Prasanna, U. R., and Rajashekara, K. (2015). Novel modular multiple-input bidirectional DC–DC power converter (MIPC) for HEV/FCV application. *IEEE Trans. Ind. Electron.* 62 (5), 3163–3172. doi:10.1109/tie.2014.2371778

Jang, Y., and Jovanovic, M. M. (2007). Interleaved boost converter with intrinsic voltage-doubler characteristic for universal-line PFC front end. *IEEE Trans. Power Electron.* 22 (4), 1394–1401. doi:10.1109/tpel.2007.900502

Jiang, L., Mi, C. C., Li, S., Zhang, M., Zhang, X., and Yin, C. (2013). A novel soft-switching bidirectional DC–DC converter with coupled inductors. *IEEE Trans. Ind. Appl.* 49 (6), 2730–2740. doi:10.1109/tia.2013.2265874

Jung, D.-Y., Hwang, S.-H., Ji, Y.-H., Lee, J.-H., Jung, Y.-C., and Won, C.-Y. (2013). Soft-switching bidirectional DC/DC converter with a LC series resonant circuit. *IEEE Trans. Power Electron.* 28 (4), 1680–1690. doi:10.1109/tpel.2012.2208765

Khaligh, A., and Li, Z. (2010). Battery, ultracapacitor, fuel cell, and hybrid energystorage systems for electric, hybrid electric, fuel cell, and plug-in hybrid electric vehicles: State of the art. *IEEE Trans. Veh. Technol.* 59 (6), 2806–2814. doi:10.1109/tvt.2010.2047877

Kharade, J. M., Patil, A. A., Yadav, N. V., Kamble, B. D., and Virbhadre, A. B. (2021). "Dual battery charger system for electric vehicle," in 2021 Second International Conference on Electronics and Sustainable Communication Systems (ICESC), Coimbatore, India, August 2021 (IEEE), 157–161. doi:10.1109/ICESC51422.2021.9532862

Krishnaswami, H., and Mohan, N. (2009). Three-port series-resonant DC–DC converter to interface renewable energy sources with bidirectional load and energy storage ports. *IEEE Trans. Power Electron.* 24 (10), 2289–2297. doi:10.1109/tpel.2009.2022756

Lai, C.-M. (2016). Development of a novel bidirectional DC/DC converter topology with high voltage conversion ratio for electric vehicles and DC-microgrids. *Energies* 9 (6), 410. doi:10.3390/en9060410

Lai, C.-M., Lin, Y.-C., and Lee, D. (2015). Study and implementation of a two-phase interleaved bidirectional DC/DC converter for vehicle and dc-microgrid systems. *Energies* 8 (9), 9969–9991. doi:10.3390/en8099969

Lai, C., Cheng, Y., Hsieh, M., and Lin, Y. (2018). Development of a bidirectional DC/DC converter with dual-battery energy storage for hybrid electric vehicle system. *IEEE Trans. Veh. Technol.* 67 (2), 1036–1052. doi:10.1109/TVT.2017.2763157

Lin, B.-R., and Chao, C.-H. (2013). Soft-switching converter with two series half-bridge legs to reduce voltage stress of active switches. *IEEE Trans. Ind. Electron.* 60 (6), 2214–2224. doi:10.1109/tie.2012.2191758

Liu, Y.-C., and Chen, Y.-M. (2009). A systematic approach to synthesizing multi-input DC–DC converters. *IEEE Trans. Power Electron.* 24 (1), 116–127. doi:10.1109/tpel.2008.2009170

Lu, Y., Liu, S., Wu, M., and Kong, D. (2021). "Energy management of dual energy sources pure electric vehicle based on Fuzzy control," in 2021 IEEE International Conference on Internet of Things and Intelligence Systems (IoTaIS), Bandung, Indonesia, November 2021 (IEEE), 228–233. doi:10.1109/IoTaIS53735.2021.9628658

Manjunatha, K. C., and Manjesh (2017). "Design and development of fly-back converter with buck-boost regulator for DC motor used in electric vehicle for the application of renewable energy," in 2017 International Conference on Circuit ,Power and Computing Technologies (ICCPCT), Kollam, India, April 2017 (IEEE), 1–4. doi:10.1109/ICCPCT.2017.8074256

Mehta, C. P., and Balamurugan, P. (2016). "Buck-Boost converter as power factor correction controller for plug-in electric vehicles and battery charging application," in 2016 IEEE 6th International Conference on Power Systems (ICPS), New Delhi, India, March 2016 (IEEE), 1–6. doi:10.1109/ICPES.2016.7584111

Monteiro, V., Ferreira, J. C., Nogueiras Meléndez, A. A., Couto, C., and Afonso, J. L. (2018). Experimental Validation of a novel architecture based on a dual-Stage converter for off-Board Fast battery Chargers of electric vehicles. *IEEE Trans. Veh. Technol.* 67 (2), 1000–1011. doi:10.1109/TVT.2017.2755545

Moradisizkoohi, C. H., Elsayad, N., and Mohammed, O. A. (2019). Experimental Verification of a double-input soft-Switched DC–DC converter for fuel cell electric vehicle with hybrid energy storage system. *IEEE Trans. Ind. Appl.* 55 (6), 6451–6465. doi:10.1109/TIA.2019.2937288

Moreno, J., Ortúzar, M. E., and Dixon, J. W. (2006). Energy-management system for a hybrid electric vehicle, using ultracapacitors and neural networks. *IEEE Trans. Ind. Electron.* 53 (2), 614–623. doi:10.1109/tie.2006.870880

Nayak, P. S. R., Kamalapathi, K., Laxman, N., and Tyagi, V. K. (2021). "Design and simulation of BUCK-BOOST type dual input DC-DC converter for battery charging application in electric vehicle," in 2021 International Conference on Sustainable Energy and Future Electric Transportation (SEFET), Hyderabad, India, January 2021 (IEEE), 1–6. doi:10.1109/SeFet48154.2021.9375658

Nguyen, H. V., To, D. -D., and Lee, D. -C. (2018). Onboard battery Chargers for plug-in electric vehicles with dual functional circuit for low-voltage battery charging and active power Decoupling. *IEEE Access* 6, 70212–70222. doi:10.1109/ACCESS.2018.2876645

Omara, A. M., and Sleptsov, M. (2016). "Bidirectional interleaved DC/DC converter for electric vehicle application," in 2016 11th International Forum on Strategic Technology (IFOST), Novosibirsk, Russia, June 2016 (IEEE), 100–104. doi:10.1109/IFOST.2016.7884201

Prajapati, Y., and Maurya, R. (2019). "Battery charging station for multiple electric vehicles with power conditioning," in 2019 IEEE 1st International Conference on Energy, Systems and Information Processing (ICESIP), Chennai, India, July 2019 (IEEE), 1–6. doi:10.1109/ICESIP46348.2019.8938243

Rahimifard, S., Habibi, S., and Tjong, J. (2020). "Dual Estimation strategy for new and aged electric vehicles batteries," in 2020 IEEE Transportation Electrification Conference & Expo (ITEC), Chicago, IL, USA, June 2020 (IEEE), 579–583. doi:10.1109/ITEC48692.2020.9161556

Rahman, M. M., Uddin, M. N., and Islam, M. K. (2015). "Performance enhancement of a bi-directional DC-DC converter using a Ćuk converter for electric vehicle applications," in 2015 IEEE 28th Canadian Conference on Electrical and Computer Engineering (CCECE), Halifax, NS, Canada, May 2015 (IEEE), 875–880. doi:10.1109/CCECE.2015.7129390

Rajashekara, K. (2013). Present status and future trends in electric vehicle propulsion technologies. *IEEE J. Emerg. Sel. Top. Power Electron.* 1 (1), 3–10. doi:10.1109/jestpe.2013.2259614

Ruan, J., and Song, Q. (2019). A novel dual-motor two-speed Direct drive battery electric vehicle Drivetrain. *IEEE Access* 7, 54330–54342. doi:10.1109/ACCESS.2019.2912994

Sakr, N., Sadarnac, D., and Gascher, A. (2015). "A new combined bidirectional boost converter and battery charger for electric vehicles," in IECON 2015 - 41st Annual Conference of the IEEE Industrial Electronics Society, Yokohama, Japan, November 2015 (IEEE), 001258–001263. doi:10.1109/IECON.2015.7392273

Schaltz, E., Khaligh, A., and Rasmussen, P. O. (2009). Influence of battery/ultracapacitor energy-storage sizing on battery lifetime in a fuel cell hybrid electric vehicle. *IEEE Trans. Veh. Technol.* 58 (8), 3882–3891. doi:10.1109/tvt.2009.2027909

Tao, H., Duarte, J. L., and Hendrix, M. A. (2008). Three-port triple-half-bridge bidirectional converter with zero-voltage switching. *IEEE Trans. Power Electron.* 23 (2), 782–792. doi:10.1109/tpel.2007.915023

Thounthong, P., Chunkag, V., Sethakul, P., Davat, B., and Hinaje, M. (2009). Comparative study of fuel-cell vehicle hybridization with battery or supercapacitor storage device. *IEEE Trans. Veh. Technol.* 58 (8), 3892–3904. doi:10.1109/tvt.2009.2028571

Trovão, J. P. F., Roux, M., Ménard, É., and Dubois, M. R. (2017). Energy- and power-Split management of dual energy storage system for a three-Wheel electric vehicle. *IEEE Trans. Veh. Technol.* 66 (7), 5540–5550. doi:10.1109/TVT.2016.2636282

Wai, R.-J., and Chen, B.-H. (2014). High-efficiency dual-input interleaved DC–DC converter for reversible power sources. *IEEE Trans. Power Electron.* 29 (6), 2903–2921. doi:10.1109/tpel.2013.2275663

Wang, W., Zhang, Z., Shi, J., Lin, C., and Gao, Y. (2018). Optimization of a dual-motor coupled Powertrain energy management strategy for a battery electric bus based on dynamic Programming method. *IEEE Access* 6, 32899–32909. doi:10.1109/ACCESS.2018.2847323

Wu, H., Sun, K., Ding, S., and Xing, Y. (2013). Topology derivation of non-isolated three-port DC–DC converters from DIC and DOC. *IEEE Trans. Power Electron.* 28 (7), 3297–3307. doi:10.1109/tpel.2012.2221746

Zhao, B., Song, Q., and Liu, W. (2012). Power characterization of isolated bidirectional dual-active-bridge DC–DC converter with dual-phase-shift control. *IEEE Trans. Power Electron.* 27 (9), 4172–4176. doi:10.1109/tpel.2012.2189586

Glossary

EV Electric Vehicle
BDCC Bidirectional DC/DC Converter
HEV Hybrid Electric Vehicle
DSP Digital Signal Processor
FCV Fuel Cell Vehicle
PHEV Plugin Hybrid electric vehicle
ESS Energy Storage System
SC Super Capacitor
MIMO Multi Input Multi Output
PI Proportional Integral
IGBT Integrated Bipolar Transistor
MOSFET Metal Oxide Semiconductor Field Effect Transistor
CCM Continuous Conduction Mode
PMSG Permanent Magnet Synchronous Generator
DP Dynamic Programming
OBC Onboard Battery Charger
LV Low Voltage
HV High Voltage
DAB Dual Active Bridge
BMS Battery Management System
SOH Stage of Health
DIBBC Dual Input Buck Boost Converter
SOC State of Charge
CB Charge Pump Capacitor
SR Synchronous Rectifier
PWM Pulse Width Modulator

List of Symbols

ES1 Primary Battery
ES2 Auxiliary/Extra Battery
$\mathbf{V_H}$ Higher Voltage Bus/DC Bus Voltage
$\mathbf{I_H}$ High side current
$\mathbf{i_{L1}}$ **&** $\mathbf{i_{L2}}$ Inductor Currents
$\mathbf{C_{L1}}$ **&** $\mathbf{C_{L2}}$ Capacitor Currents
$\mathbf{V_{ES1}}$, $\mathbf{V_{ES2}}$ Energy Storage systems
S, SES1, SES2 Bidirectional Power Switches
CB Charge Pump Capacitor
$\mathbf{D_d}$ Duty Cycle of Q_1 & Q_2
$\mathbf{D_u}$ Duty Cycle of Q_3 & Q_4
$\mathbf{V_{CB}}$ Charge Pump Capacitor Voltage
$\mathbf{P_{dem}}$ Power Demand
Q1, Q2, Q3, Q4 Switches
L1, L2 Inductors
VES1, VES2 Voltage Sources